This article has been accepted for publication in a future issue of this journal, but has not been fully edited. Content may change prior to final publication. Citation information: DOI 10.1109/ACCESS.2020.3020881, IEEE Access

IEEE Access
Multidisciplinary | Rapid Review | Open Access Journal

Magnetic anomaly signal detection using parallel monostable stochastic resonance system

Liu Wang[1], Liu Zhongyan[1], Zhang Qi[1], Xu Yujing[1], Liu Shuchang[1], Chen Zhuo[1], Zhu Canlin[1], Wang Ze[1], Pan Mengchun[1], Hu Jiafei[1], Li Peisen[1]

[1]College of Artificial Intelligence, National University of Defense Technology, Changsha 410073, China

Corresponding author: Zhang Qi (13873191345@163.com); Liu Zhongyan (liu.zhongyan2008@163.com)

ABSTRACT The nonlinear stochastic resonance (SR) system possesses the ability of taking advantage of noise to enhance the weak signal when the SR system, signal and noise reach to the matching relation. It provides an effective approach to detect the weak magnetic anomaly signal in low signal-to-noise ratio. However, in practical applications, the measured magnetic anomaly signal may be a peak signal, a trough signal, or a combination of the two due to the uncertainty of magnetic target orientation. Hence it is difficult to maintain a good detection performance with single SR system because the SR system output is directly influenced by signal waveforms. Aiming to this, a new strategy using the parallel monostable SR (PMSR) system is proposed, which can ensure the good detection performance regardless of a peak signal, a trough signal, or a combination of the two. Besides, we take the kurtosis index as the criterion and search the optimal system parameters in SR system. The simulation and experiment results indicate its availability, validity and that it can achieve a good detection performance in different waveforms. It can be expected to be widely used in the field of magnetic anomaly detection with PMSR system.

INDEX TERMS Magnetic anomaly detection, parallel monostable stochastic resonance, signal waveforms.

I. INTRODUCTION

Comparing with common target detection methods [1-3], magnetic anomaly detection is an effective method for hidden ferromagnetic target detection [4]. It possesses the advantages of good performance, crypticity and high anti-interference capability and extensively used in prospection, archaeological investigation and vehicle tracking [5-6]. However, the magnetic anomaly signal is very weak, and often buried deeply in the geomagnetic environment noise. Therefore, it needs to identify the weak magnetic anomaly signal from geomagnetic environment noise [7-9].

At present, some magnetic anomaly detection methods have been used to solve the problem, such as orthonormal basis functions (OBFs) decomposition [10], minimum entropy [11] and full connected neural network (FCN) [12]. The OBFs method is proposed by Ginzburg et al., which is designed based on signal waveforms, and has good performance when the signal is submerged in white Gaussian noise. Unfortunately, the real geomagnetic environment noise tends to be colored Gaussian noise [13]. The minimum entropy (ME) method is built by the probability density function of geomagnetic environment noise samples and considers that the changes are caused by the existence of a ferromagnetic target. However, the detection performance is constrained by the low signal-to-noise ratio (SNR). The FCN method regards the magnetic anomaly detection as a binary classification task to judge whether the anomaly signal appears or not, but the method depends on training data and lacks generalization ability.

Stochastic resonance (SR) is firstly proposed by Benzi [14]. It utilizes non-linear system to engender synergy between the signal and the noise when the system structural parameters are appropriate [15]. More specifically, SR can take advantage of noise to enhance the target signal, which provide a way for weak signal detection in low SNR. Wan [16] firstly introduced the SR system into the field of magnetic anomaly signal detection and the results show that the SR system can achieve higher detection probability than traditional methods under the same basis. But only one SR system is used in [16], which is effective in detecting the specific part (peak or trough) of magnetic anomaly signal. In fact, the measured magnetic anomaly signal may be a peak signal, a trough signal or the combination of the two due to the uncertainty of magnetic target orientation [17]. Hence it is difficult for single SR system to perform well in practical application.

This paper aims to present a parallel monostable stochastic resonance (PMSR) system to realize the magnetic anomaly signal detection regardless of a peak signal, a trough signal, or a combination of the two. Firstly, the magnetic anomaly detection model is introduced. Secondly, we present the detection theory of monostable SR system and design a

This article has been accepted for publication in a future issue of this journal, but has not been fully edited. Content may change prior to final publication. Citation information: DOI 10.1109/ACCESS.2020.3020881, IEEE Access

PMSR system for magnetic anomaly signal detection, in which the kurtosis index is used to adjust the system parameters according to the system input. Finally, the simulation and experiment are conducted, in which we analyze the performance of PMSR detector in different magnetic anomaly signal waveforms.

II. Magnetic anomaly signal

In the magnetic anomaly detection model [18], the visually obscured ferromagnetic objects usually can be regarded as a magnetic dipole and the magnetic field $\boldsymbol{B}_r$ produced by it can be described as follows

$$\boldsymbol{B}_r = \frac{\mu}{4\pi}\left[\frac{3(\boldsymbol{M}\cdot\boldsymbol{r})\boldsymbol{r}}{|\boldsymbol{r}|^5} - \frac{\boldsymbol{M}}{|\boldsymbol{r}|^3}\right] \tag{1}$$

where μ is space permeability, $\boldsymbol{M}$ is the magnetic moment of the dipole, $\boldsymbol{r}$ is the displacement vector between measurement point and magnetic dipole, $|\boldsymbol{r}|$ is the modulus of $\boldsymbol{r}$.

In fact, the measured magnetic field consists of geomagnetic field $\boldsymbol{T}$ and anomaly field $\boldsymbol{B}_r$ generated by ferromagnetic object. When $|\boldsymbol{T}| >> |\boldsymbol{B}_r|$, the magnetic anomaly signal S_r can be expressed by

$$S_r = \frac{\boldsymbol{B}_r \cdot \boldsymbol{T}}{|\boldsymbol{T}|} \tag{2}$$

The magnetic anomaly detection model is shown in Fig.1, the magnetic dipole (target) with the moment of $\boldsymbol{M}$ lies at origin O of the Cartesian coordinate system, in which the *X*-axis orients towards the magnetic North, the *Y*-axis orients towards East, and the *Z*-axis orients upwards. The sensor moves horizontally in a straight line with the relative angle θ between the search path and *X*-axis, l is horizontal component of nearest distance between the search path and origin, and h is the vertical component. v represents the moving speed of the sensor.

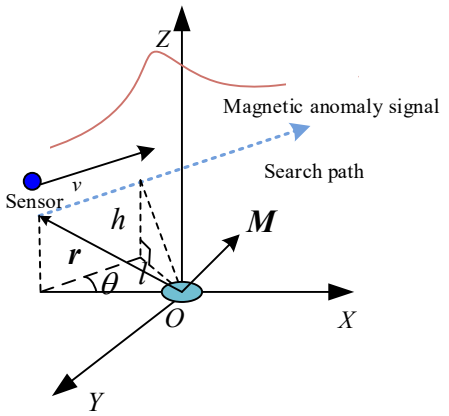

FIGURE 1. Diagram of magnetic anomaly target detection model.

In the process of searching, from approaching the target, passing through the target, and to leaving the target, the measured magnetic signal will change obviously in the amplitude due to the existence of the target. Fig.2 shows the typical waveforms of magnetic anomaly signal in different relative angle θ. It is obvious that the magnetic anomaly signal is the aperiodic impact signal, which is represented as peak, trough, or the mixture of the two.

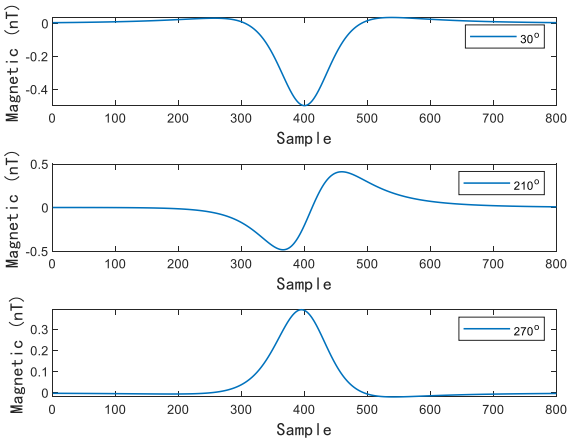

FIGURE 2. Typical magnetic anomaly signal.

III. Detection theory

A. Principle of monostable stochastic resonance

The magnetic anomaly signal is a typical impact signal. For impact signal detection, the monostable SR system which is shown in Fig.3 is usually used [19] and can be described by nonlinear Langevin Equation as follows

$$x'(t) = -V'(x) + s(t) + \xi(t) \tag{3}$$

where $x(t)$ is the response of SR system, $x'(t)$ is the time derivative of $x(t)$, $s(t)$ is the signal and $\xi(t)$ is the noise with zeros mean. In our study, $s(t)$ represents the magnetic anomaly signal, $\xi(t)$ represents the geomagnetic noise. $V'(x)$ is the time derivative of $V(x)$, which is named as nonlinear potential function and is expressed as

$$V(x) = -ax + bx^4/4 \tag{4}$$

where a, b are the system parameters of the nonlinear system, and $b > 0$. The discretization of equation (3) and (4) can be solved by using a fourth order Runge-Kutta method [14].

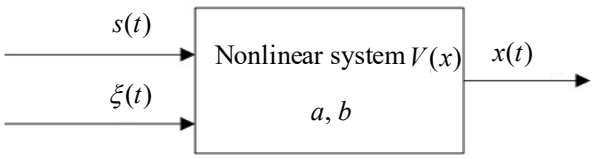

FIGURE 3. The input and response of monostable SR system.

Fig.4 shows the potential function (top) and response (bottom) of monostable SR system with different a. It is calculated that the system only has a stable point in $x_{\min} = \sqrt[3]{a/b}$. When $a < 0$, the curve left to $x_{\min}$ is steeper than that in the right, so the positive part (peak) of signal

This article has been accepted for publication in a future issue of this journal, but has not been fully edited. Content may change prior to final publication. Citation information: DOI 10.1109/ACCESS.2020.3020881, IEEE Access

will be magnified with the drive of the noise, which means that the system is more sensitive to peak signal. Similarly, when $a>0$, the system is more sensitive to trough signal. More principle analysis about monostable SR system can refer to literature [19].

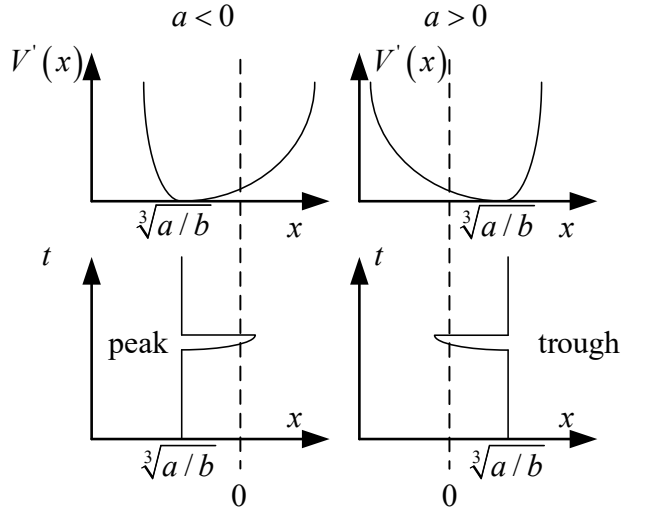

FIGURE 4. The potential function (top) and system response (bottom) in monostable SR system with different a.

The introduction above reveals that the monostable SR system is effective in detecting the specific part (trough or peak) of the signal, which depends on the choice of system parameter a. However, the trough or peak part of magnetic anomaly signal is usually unknown, and single monostable SR system may not be effective enough for magnetic anomaly detection in practical application. So a new strategy using the PMSR system is proposed to solve these problems.

B. PMSR system for magnetic anomaly detection

As is shown in Fig.5, the PMSR system consists of two monostable SR subsystems, named as SR^+ and SR^-. The monostable SR system combined with the receiver where the standard deviation (*std*) is treated as the binary hypothesis testing statistic quantity, is named as a detector. SR^+ detector is for peak signal detection and SR^- detector is for trough signal detection. The complete detection process is introduced as follows:

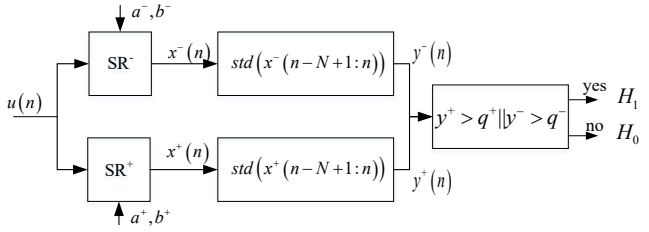

FIGURE 5. The detection diagram of PMSR system.

Firstly, the SR^+ system parameters a^+,b^+ and SR^- system parameters a^-,b^- will be selected appropriately to make sure that both subsystems work in good condition.

Secondly, the measurement signal $u(n)$ will be sent to PMSR system, $x^+(n),x^-(n)$ are the system responses. $y^+(n),y^-(n)$ are the receiver outputs, which are calculated by

$$\begin{cases} y^+(n)=std\left(x^+(n-N+1:n)\right) \\ y^-(n)=std\left(x^-(n-N+1:n)\right) \end{cases} \tag{5}$$

where *std* means the standard deviation of x between $n-N+1$ and n, N is the length of moving window.

Finally, the Neyman–Pearson (NP) criterion [20] is applied to choose the judgement threshold q^+,q^-, which are used to judge the anomaly target. If $y^->q^-$ or $y^+>q^+$, it is considered that a magnetic anomaly object occurs, which is represented by H_1. H_0 represents the hypothesis of noise only.

When the SR system, input signal and noise reach to some matching relationship, the weak input signal will get highly enhanced by the noise. However, the matching relation cannot be reached all the time when the system parameters a,b are inappropriate. So it is necessary to select appropriate parameters for the system.

C. System parameters selection

As we know, the magnetic anomaly signal is a typical impact signal, and the kurtosis index (K) is usually used to evaluate impact signal [21]. The more obvious the impact component is, the larger the kurtosis index is. K is defined as the ratio of the fourth-order moment and the second-order moment (variance) square of the signal as follows [22]:

$$K=\frac{1}{N}\sum_{i=1}^{N}(x_i-\bar{x})^4 \Big/ \left[\frac{1}{N}\sum_{i=1}^{N}(x_i-\bar{x})^2\right]^2 \tag{6}$$

where x_i represents signal sequence, $\bar{x}$ represents the mean value of signal sequence, N is the length of signal sequence.

In our study, the environment noise can be sampled in advance, and typical peak or trough signal combined with the noise will be sent to corresponding SR system. Then the kurtosis K of system response will be calculated when using the system parameters a,b, and the purpose is to find the a,b corresponding to the maximum $K(a,b)$, which can be described by

$$\begin{aligned} &\left(a^*,b^*\right)=\arg\max K(a,b) \\ &s.t.\ \ a\in[a_{\min},a_{\max}],b\in[b_{\min},b_{\max}] \end{aligned} \tag{7}$$

where $a_{\min},a_{\max},b_{\min},b_{\max}$ represent the searching range of a,b and a^*,b^* are the searching result. After setting the range and step of a,b, equation (7) can be solved by the searching algorithm and the appropriate system parameters will be obtained.

IV. Simulation

This article has been accepted for publication in a future issue of this journal, but has not been fully edited. Content may change prior to final publication. Citation information: DOI 10.1109/ACCESS.2020.3020881, IEEE Access

A. Simulation method

Firstly, the magnetic anomaly signal is generated by the detection model which is introduced in Fig.1. The model parameters setting is shown in Table.1. By changing the relative angles θ, we can obtain the magnetic anomaly signal with different waveforms. In the simulation, three typical signals (peak, trough and mixed signal) will be generated. The noise used in simulation is a random sample from $1/f^{\alpha}$ colored Gaussian noise [23], α is noise exponent. α=0.8 is used to generate the noise because α of real noise is about 0.8-1.2 [16]. The standard deviation of noise is 0.16nT and the range is about [-0.4nT, 0.4nT]. The sampling frequency is f_s=20Hz.

TABLE 1. Parameters setting of detection model.

$\boldsymbol{T}$	θ	v
(3.1, -0.2, 3.5) $\times 10^4$ nT	30°, 210°, 270°	100 m/s
$\boldsymbol{M}$	l	h
(1.5, 0.4, 1.4)$\times 10^5$ A·m^2	420 m	200 m

Secondly, the typical peak or trough signal with noise are used to obtain the structural parameters with the application of kurtosis. According to the practical experience, for SR^+ system parameters a^+, b^+, the value ranges are usually [-1, 0], [0, 40] respectively, and for SR^- system parameters a^-, b^-, the value ranges are usually [0, 1], [0, 40] respectively.

Finally, three typical signals contaminated by noise are used as the input of PMSR detector. Monte Carlo method [24] is applied to test the performance of the detector, in which 10000 detections repeat under the same hypothesis. In each repeating detection, the noise is a random sample from the simulation noise. The threshold value q^+, q^- are determined by using the Neyman–Pearson criterion under a limitation on the false alarm rate 1.5% [25-27].

B. Simulation results in different waveforms

Fig.6 shows the results of PMSR detector in peak signal detection. Fig.6 (a), (b) show the peak signal and the peak signal contaminated by noise respectively. Fig.6 (c), (d) show the responses of SR^- and SR^+ system. By comparing the system input (b) and system response (c), it indicates that the anomaly signal is greatly enhanced and the SNR has a significant improvement. Fig.6 (e), (f) represent the outputs of SR^- and SR^+ receiver, which are calculated by equation (5) with the moving windows length 200 and the red line means the threshold value. It reveals that the magnetic anomaly signal is detected by SR^+ detector (Fig.6 (f)) because of the high output amplitude in corresponding position. Fig.7 shows the results of PMSR detector in trough signal detection. It can be seen that only the output of SR^- detector reveals the exitance of anomaly signal (Fig.7 (e)). Fig.8 shows the results of PMSR detector in the mixed signal detection. According to Fig.8 (e), (f), the anomaly signal is detected by both SR^+ and SR^- detector.

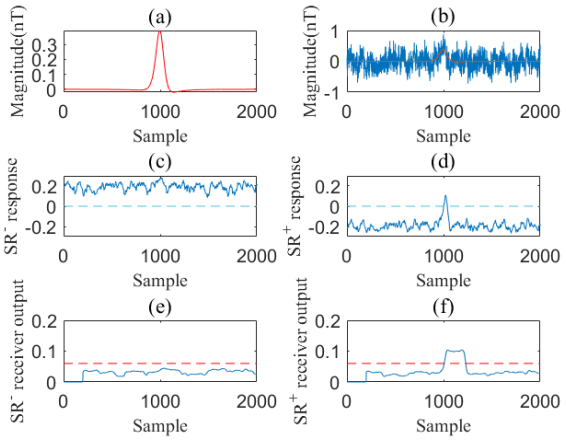

FIGURE 6. Results of PMSR detector in peak signal.
(a) Peak signal. (b) Peak signal with noise. (c) SR⁻ system response. (d) SR⁺ system response. (e) SR⁻ receiver output. (f) SR⁺ receiver output.

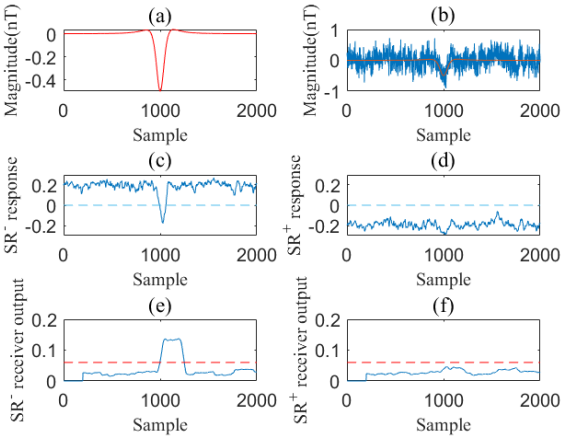

FIGURE 7. Results of PMSR detector in trough signal.
(a) Trough signal. (b) Trough signal with noise. (c) SR⁻ system response. (d) SR⁺ system response. (e) SR⁻ receiver output. (f) SR⁺ receiver output.

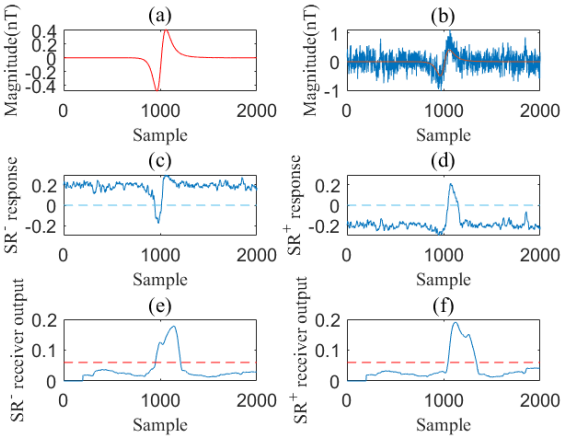

FIGURE 8. Results of PMSR detector in mixed signal.
(a) Mixed signal. (b) Mixed signal with noise. (c) SR⁻ system response. (d) SR⁺ system response. (e) SR⁻ receiver output. (f) SR⁺ receiver output.

The above results demonstrate that single SR detector is only effective in detecting the specific part (peak or trough) of the signal, but the PMSR detector can overcome the

This article has been accepted for publication in a future issue of this journal, but has not been fully edited. Content may change prior to final publication. Citation information: DOI 10.1109/ACCESS.2020.3020881, IEEE Access

shortage of single detector and is more applicable in detecting the magnetic anomaly signal with different waveforms.

C. Performance comparison with single SR detector

To evaluate the detection probability of the PMSR detector, a statistical test have been given out, in which we compare the performance of the proposed method with single SR^{+}, SR^{-} detector under different waveforms and different SNRs. The SNR is defined by

$$\mathrm{SNR} = 10\log_{10}\frac{\frac{1}{N}\sum_{i=1}^{N}s(i)}{\frac{1}{G}\sum_{j=1}^{G}\left(\frac{1}{N}\sum_{i=1}^{N}\xi_j(i)\right)} \tag{8}$$

where s is the anomaly signal and ξ is the environment noise, N means the length of moving window, G is the repeated sampling times of the noise. It is important to note that we obtain the sample of detector input under different SNRs by changing the amplitude of the magnetic anomaly signal. The detection probability is obtained by using Monte Carlo method with 10000 detections repeat under the same hypothesis.

Fig.9 (a) shows the detection probability of three detectors in peak signal. It is found that the detection probability of PMSR detector is about 0.81-1 between -3dB and 0dB, and SR^{+} detector has similar performance compared with PMSR detector, but SR^{-} detector has bad performance. Fig.9 (b) shows the detection probability of three detectors in trough signal. The PMSR detector and SR^{-} detector almost has the same detection probability which is about 0.80 in -3dB, while SR^{+} detector performs badly. Fig.9 (c) shows the detection probability of three detector in mixed signal. It is obvious that the PMSR detector can keep the high detection probability no matter what waveform the signal is.

According to the analysis above, it can be known that the PMSR detector can maintain a good detection performance in different waveforms, and single SR detector may performs badly when detecting the signal with specific waveforms. So the PMSR detector has a more extensive application prospect.

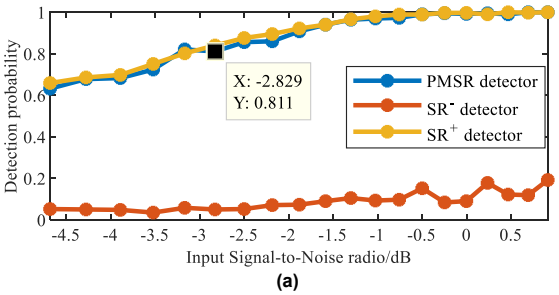

(a)

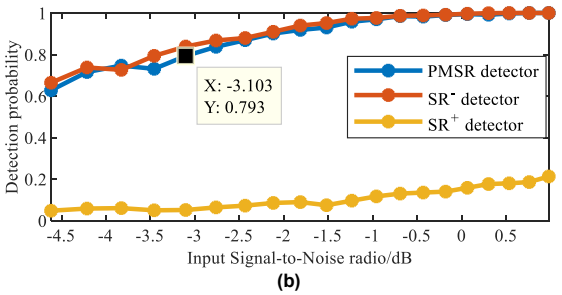

(b)

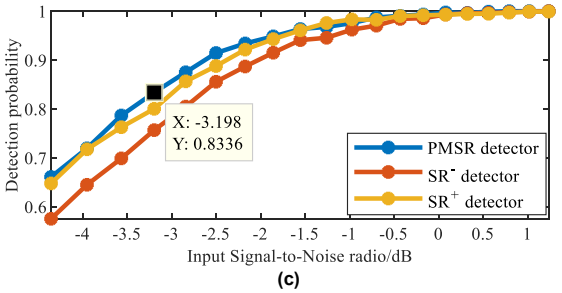

(c)

FIGURE 9. Detection probability of PMSR detector in different waveforms under simulation noise. (a) peak signal detection. (b) trough signal detection. (c) mixed signal detection.

V. Experiment

A. Experiment design

In order to verify the effectiveness of the PMSR detector in real noise, we conduct an experiment to acquire the noise. As shown in Fig.10, the real noise is measured by AARC510/CS-VL optical pump magnetometer [28] in the field. The sensitivity of magnetometer CS-VL is $0.6\mathrm{pT}/\sqrt{\mathrm{Hz}}$ (root mean square) and the intrinsic noise is $<2\mathrm{pT}$ (peak to peak value). The output of CS-VL is sampled by data acquisition device AARC510 with the sampling frequency of 20Hz. Besides, the measurement signal contains background geomagnetic and it is necessary to remove the trend and bias of the geomagnetic so that we can obtain the real noise needed. In addition, the magnetic anomaly signal is generated by detection model which is introduced in Fig.1. Three typical signals (Fig.2) contaminated by real noise are considered as the detector input. The process of system parameters selection and threshold determination is similar to the simulation.

B. Real noise analysis

Fig.11 (a) shows a fragment of measurement geomagnetic with the length of 10000, which contains the geomagnetic noise and the sensor noise. After removing the trend and bias of real geomagnetic [16], the remnant is considered as the real magnetic noise which is shown in Fig. 11(b), the standard deviation is 0.17nT, the kurtosis is 3.2 (3 for white Gaussian noise), the skewness is -0.05 (0 for white Gaussian noise) and the range is about (-0.5nT, 0.5nT). Fig.11(c) shows the power spectral density of real noise, it is calculated that the noise exponent is between 0.7 and 1.0. Next the real noise will be added in the typical signal to test the performance of proposed method.

This article has been accepted for publication in a future issue of this journal, but has not been fully edited. Content may change prior to final publication. Citation information: DOI 10.1109/ACCESS.2020.3020881, IEEE Access

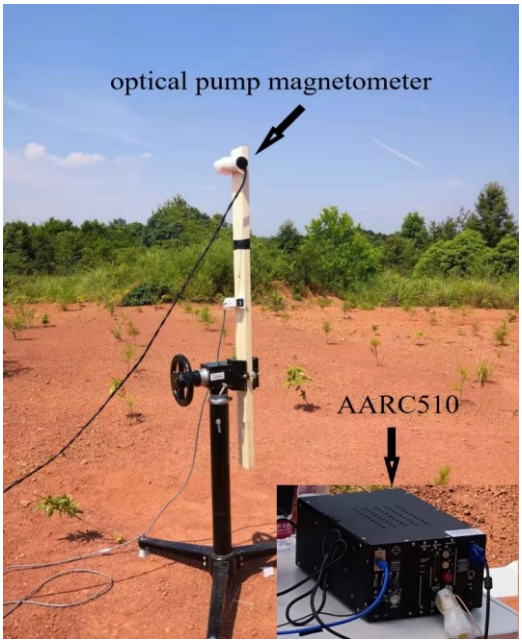

FIGURE 10. The scene of measurement

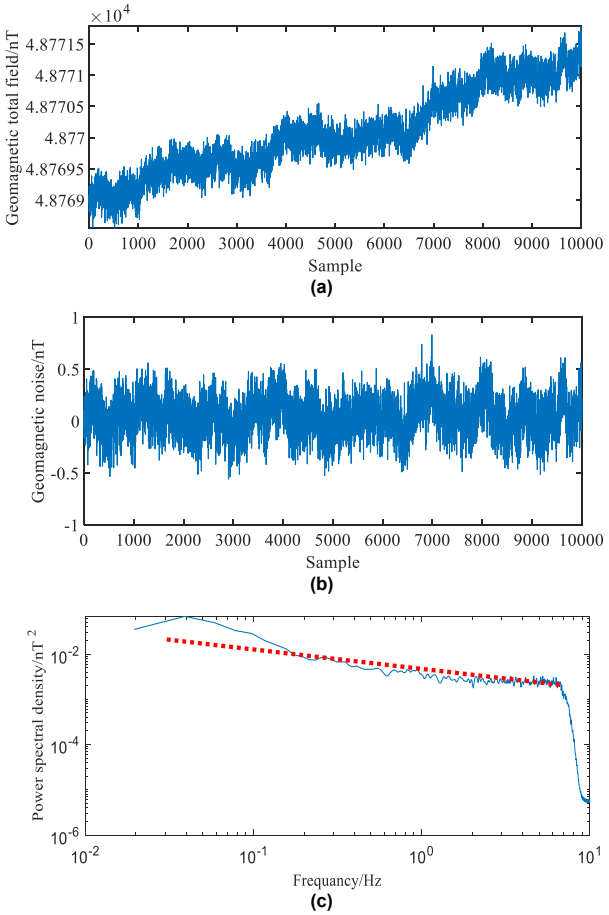

FIGURE 11. Measurement results.
(a) Real geomagnetic. (b)Real noise after detrending. (c) Power spectral density of real noise.

C. Results of PMSR detector in real noise

Fig.12 show the results of the proposed detector in real noise, Fig12 (a), (b), (c) represent the typical peak, trough and mixed signal contaminated by real noise respectively. Fig. 12 (d), (e), (f) show the SR^- detector outputs and Fig. 12 (g), (h), (i) show the SR^+ detector outputs. It can be seen that the signal is obliterated by the real noise, but detected by the proposed method. The peak signal is detected by SR^+ detector (Fig.12 (g)), and the trough signal is captured by SR^- detector (Fig.12 (e)), and both detectors performs well in mixed signal detection (Fig.12 (f), (i)). All the results reveal that the PMSR detector is effective in detecting the magnetic anomaly signal with different waveforms in real noise. The experiment results are basically consistent with the simulation results.

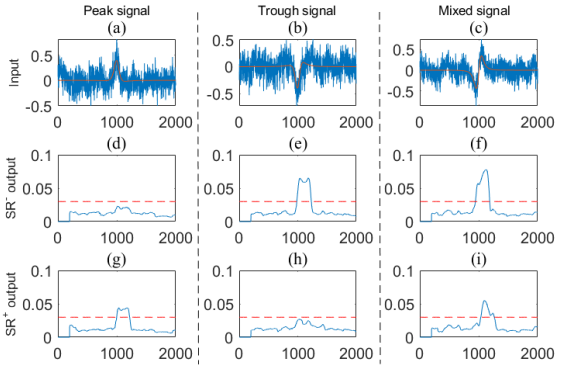

FIGURE 12. Results of PMSR detector in real noise.
(a) Peak signal with noise. (b) Trough signal with noise. (c) Mixed signal with noise. (d) SR^- detector output of peak signal. (e) SR^- detector output of trough signal. (f) SR^- detector output of mixed signal. (g) SR^+ detector output of peak signal. (h) SR^+ detector output of trough signal. (i) SR^+ detector output of mixed signal.

In order to further compare the performance of three detectors in different waveforms, we design a statistic test, in which 12 different relative angles is selected to generate the magnetic anomaly signal with different waveforms. Monte Carlo method with 10000 repetitions in the same condition is also applied to obtain the detection probability. The input SNR is about -3dB.

Fig.13 shows the detection probability of three detectors in 12 relative angles. It is obvious that the SR^- detector has high detection probability when the relative angles are between 30°-180°, in which the trough part dominates the signal. The SR^+ detector performs well in 210°-330°, because the peak part dominates the signal. However, single SR detector may have bad performance at a specific angle region. The results of PMSR detector show its detection stability in different waveforms, and maintain high detection probability, which has a wider application prospect in real magnetic anomaly detection.

This article has been accepted for publication in a future issue of this journal, but has not been fully edited. Content may change prior to final publication. Citation information: DOI 10.1109/ACCESS.2020.3020881, IEEE Access

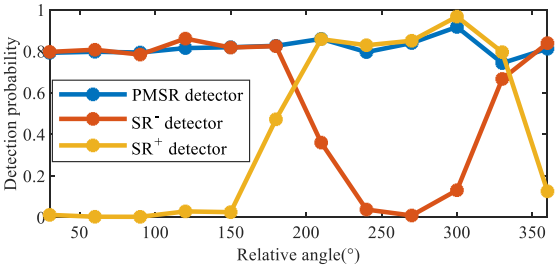

FIGURE 13. Detection probability of three detectors in real noise.

VI. Conclusion

In this paper, we proposed a method of magnetic anomaly detection based on PMSR system, which is named as PMSR detector. Firstly, the model of magnetic anomaly detection is introduced. Secondly, the structure of PMSR detector and the choice of the system parameters are described. Finally, The simulation and experiment are conducted, in which we compare the performance between PMSR detector and single monostable SR detector. The results shows that the proposed method can overcome the shortages of single monostable SR detector and maintain the detection performance in different waveforms.

References

[1] L. Wan, X. Kong, F. Xia, "Joint Range-Doppler-Angle Estimation for Intelligent Tracking of Moving Aerial Targets," IEEE Internet of Things Journal. pp.1-1. 2017.
[2] F. Wen, Z. Zhang, K. Wang, "Angle estimation and mutual coupling self-calibration for ULA-based bistatic MIMO radar," Signal Processing. pp.61-67, 2017.
[3] X. Wang, L. Wang, X. Li, "Nuclear norm minimization framework for DOA estimation in MIMO radar," Signal Processing, pp.147-152, 2017.
[4] J. E. McFee and Y. Das, "Locating and identifying compact ferrous objects," IEEE Trans. Geosci. Remote Sensing, vol.28, no.2, pp.182–193, Mar. 1990.
[5] D. Liu, X. Xu, C. Fei, "Direction identification of a moving ferromagnetic object by magnetic anomaly," Sens. Actuators A, Phys., pp. 147–153, 2015.
[6] M. Munschy, and S. Fleury, "Scalar, vector, tensor magnetic anomalies: measurement or computation?" Geophysical Prospecting, vol.59, no.6, pp.1035-1045, 2011.
[7] Z. Liu, H. Pang, M. Pan, and C. Wan, "Calibration and compensation of geomagnetic vector measurement system and improvement of magnetic anomaly detection," IEEE Geosci. Remote Sens. Lett., vol. 13, no.3, pp.447–451, Mar. 2016.
[8] C. Wan, M. Pan, "Performance improvement of magnetic anomaly detector using Karhunen-Loeve expansion," IET Sci. Meas. Technol, vol.11, pp.600-606, 2017.
[9] Y. Tang, Z. Liu, M. Pan, Q. Zhang, C. Wan, F. Guan, F. Wu, and D. Chen, "Detection of magnetic anomaly signal based on information entropy of differential signal," IEEE Geosci. Remote Sens. Lett, vol. 15, no.4, pp.512–516, Mar. 2018.
[10] B. Ginzburg, L. Frumkis, and B. Kaplan, "Processing of magnetic scalar gradiometer signals using orthonormalized functions." Sensors & Actuators A, vol.102, no.1-2, pp.67-75, 2002.
[11] A. Sheinker, N. Salomonski, B. Ginzburg, L. Frumkis, and B.-Z. Kaplan, "Magnetic anomaly detection using entropy filter," Meas. Sci. Technol. vol.19, pp.045205 (5pp), Feb.2008.
[12] S. Liu, Z. Chen, M. Pan, "Magnetic anomaly detection based on full connected neural network," IEEE Access, vol.7, pp.182198-182206, 2019.
[13] D. Liu, X. Xu, and C. Huang, "Adaptive cancellation of geomagnetic background noise for magnetic anomaly detection using coherence," Meas. Sci. Technol., vol.26, no.1, pp.015008-1–015008-6, Dec. 2015.
[14] R. Benzi, A. Sutera, A. Vulpiani, "The mechanism of stochastic resonance," Journal of physics A-Mathematical and general Journal vol.14, no.11, pp.L453, 1981.
[15] L. Gammaitoni, "Stochastic Resonance: A remarkable idea that changed our perception of noise," European Physical Journal B vol.69, no.1, pp.1-3, 2009.
[16] C. Wan, M. Pan, "Magnetic anomaly detection based on stochastic resonance," Sensors & Actuators A Physical, vol.278, pp.11-17,2017.
[17] Y. Huang, Y. Hao, "Method of separating dipole magnetic anomaly from geomagnetic field and application in underwater vehicle localization," Proc. of the 2010 IEEE Int. Conf. on Information and Automation, Harbin, China, pp.1357–1362, 2010.
[18] Y. Liu, Z Liu, M. Pan, "Magnetic Anomaly Signal Space Analysis and Its Application in Noise Suppression," IEEE Geosci. Remote Sens. Lett, vol.16, no.1, pp.130-134, 2019.
[19] Y. Leng,Y. Zhao, "Study on impulse response of monostable system," (in Chinese), Acta Phys. Sin. vol.64, no.21, 2015.
[20] S.Bayram, S.Gultekin, "Noise enhanced hypothesis-testing according to restricted Neyman–Pearson criterion," Digital Signal Processing, vol.25, pp.17-27, 2014.
[21] J. Li, X. Chen, "Adaptive Monostable Stochastic Resonance Based on PSO with Application in Impact Signal Detection," CHIN J MECH ENG-EN, vol.47, no.21, pp.210503(1-10), 2011.
[22] L.T. DeCarlo. "On the Meaning and Use of Kurtosis," Psychological Methods, vol.2, no.3, pp.292-307,1997.
[23] A. Sheinker, A. Shkalim, N. Salomonski, B. Ginzburg, L. Frumkis, and B.-Z. Kaplan, "Processing of a scalar magnetometer signal contaminated by 1/f noise," Sens. Actuators A, vol. 138, pp. 105–111, Jul. 2007.
[24] K. Mosegaard and M. Sambridge, ''Monte Carlo analysis of inverse problems,'' Inverse Problems, vol. 18, no. 3, pp. R29–R54, Apr. 2002.
[25] J. Zheng, H. Liu, Q. H. Liu, "Parameterized centroid frequency-chirp rate distribution for LFM signal analysis and mechanisms of constant delay introduction," IEEE Transactions on Signal Processing, vol.65, no.24, pp.6435-6447, 2017.
[26] J. Zheng, T. Yang, H. Liu, "Efficient Data Transmission Strategy for IIoTs with Arbitrary Geometrical Array," IEEE Transactions on Industrial Informatics, DOI 10.1109/TII.2020.2993586.
[27] J. Zheng, T. Yang, H. Liu, L. Wan, "Accurate Detection and Localization of UAV Swarms-Enabled MEC System," IEEE Transactions on Industrial Informatics, DOI10.1109/TII.2020. 3015730.
[28] Optical pump magnetometer CS-VL. [Online] . Available: https://www.Laureltechno-logies.com/zh-hant/products/cs-vl.